

# Pharmaceutical and Non-Pharmaceutical Interventions for Controlling the COVID-19 Pandemic

Jeta Molla<sup>1,2,3,\*</sup>, Suzan Farhang-Sardroodi<sup>2,3,4,\*</sup>, Iain R Moyles<sup>1,2,3,+</sup>, and Jane M Heffernan<sup>1,2,3</sup>

<sup>1</sup>Department of Mathematics and Statistics, York University, Toronto, Ontario, Canada

<sup>2</sup>Centre for Disease Modelling (CDM), Mathematics Statistics, York University, Toronto, Ontario, Canada

<sup>3</sup>Modelling Infection and Immunity Lab, Mathematics Statistics, York University, Toronto, Ontario, Canada

<sup>4</sup>Department of Mathematics, University of Manitoba, Winnipeg, Manitoba, Canada

\*Equal contribution as first author

+imoyles@yorku.ca

April 1, 2023

## Abstract

Disease spread can be affected by pharmaceutical (such as vaccination) and non-pharmaceutical interventions (such as physical distancing, mask-wearing, and contact tracing). Understanding the relationship between disease dynamics and human behavior is a significant factor to controlling infections. In this work, we propose a compartmental epidemiological model for studying how the infection dynamics of COVID-19 evolves for people with different levels of social distancing, natural immunity, and vaccine-induced immunity. Our model recreates the transmission dynamics of COVID-19 in Ontario up to December 2021. Our results indicate that people change their behaviour based on the disease dynamics and mitigation measures. Specifically, they adapt more protective behaviour when the number of infections is high and social distancing measures are in effect, and they recommence their activities when vaccination coverage is high and relaxation measures are introduced. We demonstrate that waning of infection and vaccine-induced immunity are important for reproducing disease transmission in Fall 2021.

**Keywords:** SIR Model, COVID-19, Physical Distancing, Pharmaceutical (Vaccination) and Non-Pharmaceutical Interventions, Waning Immunity

## 1 Introduction

Coronavirus disease 2019 (COVID-19) has been a global challenge leading to millions of infections and thousands of deaths globally. Before the availability of vaccines, most countries relied solely on the implementation of a range of non-pharmaceutical interventions (NPIs) such as partial closings of business, lock-downs, and mask-wearing to curb the spread of SARS-CoV-2 and avoid overburdening healthcare systems [1–3]. With the development of COVID-19 vaccines, policy makers started vaccination campaigns with the aim to protect individuals and relax NPIs. Vaccines became the most important

34 intervention for mitigating disease severity and spread, allowing the return of social and economic activ-  
35 ities [4–8].

36 Human behaviour plays an important role on the efforts to control the transmission of the COVID-19  
37 virus, since the effectiveness of mitigation measures depends on NPI compliance and vaccine acceptance.  
38 People are most likely to adapt protective behaviour when mortality or the perception of risk is high, and  
39 resume normal life as the perceived risk declines [9–11]. Hence, it is crucial to consider the effects of  
40 behaviour change over time so that the design of effective infection mitigation policies can be achieved.

41 Since the onset of the COVID-19 pandemic, many studies have developed mathematical models to  
42 describe the dynamics of transmission of the disease [12–14]. Many of the proposed models are ex-  
43 tensions of the classical Kermack-McKendrick Susceptible-Infectious-Recovered (SIR) epidemic model  
44 [15], which predicts the number of individuals who are susceptible to infection, actively infected, or  
45 have recovered from infections at any given time [16]. Several studies have extended the SIR model  
46 by considering additional compartments to account for asymptomatic cases, hospitalizations, quaran-  
47 tine, vaccination, disease induced death and /or heterogeneity of the population [17]. These epidemic  
48 models can also be coupled with models describing behaviors that are affected by and affect the disease  
49 transmission dynamics [18, 19]. Some the proposed COVID-19 compartmental models have considered  
50 how individuals respond to the disease dynamics and how the disease dynamics are affected by these  
51 behavioural responses [20–30].

52 In this study, we extend a compartmental SEPIR model first published by Moyles et al. [20]. The  
53 model divides the population into five possible disease states: Susceptible ( $S$ ), Exposed ( $E$ ), Pre-  
54 symptomatic ( $P$ ), Infected ( $I$ ) (both symptomatic  $I_S$  and asymptomatic  $I_A$ ), and Recovered ( $R$ ). It  
55 also includes three classes of social distancing over each disease state. Additionally, infections are delin-  
56 eated into those that are known and unknown. The model was used to study the first several months of  
57 the COVID-19 pandemic, and NPI compliance in Ontario, Canada. However, Moyles et al. [20] did not  
58 include vaccination, waning immunity, or viral variants as these were concerns after publication of their  
59 work. The main purpose of our study is to adapt their model to include vaccination, which confers some  
60 immunity to the disease, and waning from all sources of immunity. The effects of waning immunity have  
61 been incorporated in some epidemiological models of the COVID-19 pandemic [8, 31–35]. Furthermore,  
62 we extend the model to include variants of concern by allowing modification of the transmissibility of  
63 the disease over time. We do not include the Omicron variant in our study since data acquisition became  
64 more difficult as governments reduced testing and started lifting NPIs.

65 Since vaccination is imperfect, we introduce a complimentary compartment  $S^w$  for those who have  
66 received vaccines, but do not gain immunity. This class represents a non-existent but perceived immunity  
67 to the disease and as such we modify the model to account for a change in behaviour related to NPIs as  
68 a consequence. This compartment will also be a transient compartment for people who have waning  
69 immunity as there will be misalignment between when the protection from vaccine has diminished and  
70 when it has been perceived to have diminished.

71 To the best of our knowledge, no previous studies have studied the coupled effects of dynamic social  
72 distancing and cost-based relaxation, waning immunity, vaccination, and new variants of concern on  
73 the progression of the pandemic. Our study is organized as follows. In Section 2.1 we introduce the  
74 extended SEPIR model including new parameters, values for which are derived from existing literature  
75 or fit to data from Public Health Ontario (PHO) [36, 37]. We then present the estimated parameters  
76 using time horizons of public policy implementations in Ontario developed by Dick [38]. Additionally,  
77 we investigate the effect of waning immunity. We compare our results to publicly accessible data on

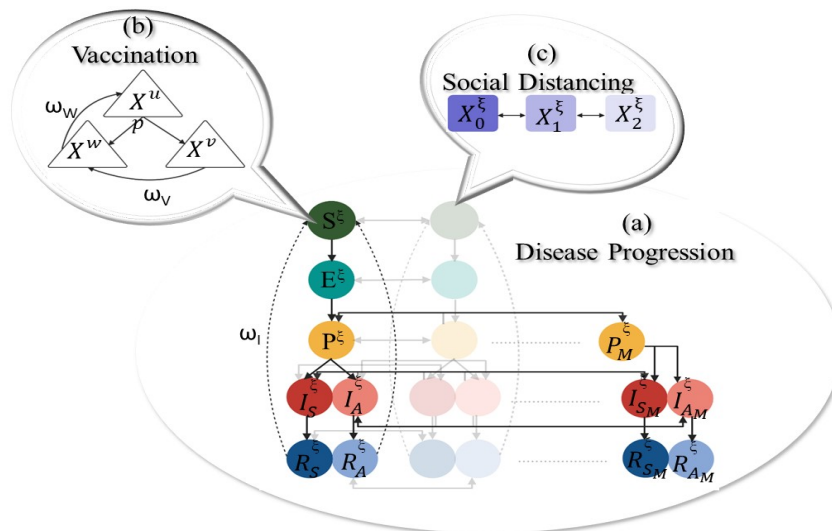


Figure 1: Schematic representation of the Susceptible- Exposed - Pre-symptomatic Infectious - Infectious Asymptomatic - Infectious Symptomatic - Recovered (SEPIR) with three levels of social distancing from no social distancing (subscript 0) to full isolation (subscript 2) (Panel (c)), and null, vaccine-induced or perceived immunity (Panel (b), superscript  $\xi = u, v, w$ ).  $X^\xi = [S^\xi, E^\xi, P^\xi, P_M^\xi, I_S^\xi, I_{S_M}^\xi, I_A^\xi, I_{A_M}^\xi, R_S^\xi, R_A^\xi, R_{S_M}^\xi, R_{A_M}^\xi]$ . Known infections (via testing) are shown with subscript  $M$ .

78 positivity rate, daily incidence and seroprevalence [36, 39]. Following Moyles et al., [20], we focus our  
 79 work on the Canadian province of Ontario. We discuss the conclusions of our work in Section 4.

## 80 2 Methods

### 81 2.1 SEPIR Model

82 We developed a compartmental mode based on the model proposed by Moyles et al. [20] which al-  
 83 lows the various classes to change transmission dynamics through isolation and contact reduction. The  
 84 Moyles et al. model is depicted in Figure 1, Panels (a) and (c). We extend the model to include vaccine-  
 85 induced immunity, and perceived immunity (shown in Panel (b)) and waning immunity. Briefly, Panel (a)  
 86 shows disease progression from susceptible ( $S$ ) to recovered ( $R$ ) through the different infection stages:  
 87 non-infectious ( $E$ ), pre-symptomatic infectious ( $P$ ), asymptomatic infectious ( $I_A$ ), and symptomatic in-  
 88 fectionous ( $I_S$ ). Reported infections are denoted with subscript  $M$ . A natural waning immunity rate  $\omega_I$   
 89 indicates the fraction of the recovered population that can once again become susceptible. Superscript  
 90  $\xi$  is shown in Panel (b) which illustrates the transition between individuals that are unvaccinated ( $u$ ),  
 91 vaccinated ( $v$ ), or with perceived immunity ( $w$ ).  $p$  is the rate of vaccination,  $\omega_V$  is the waning rate from  
 92 vaccine induced immunity, and  $\omega_W$  it the waning rate of perceived immunity. Panel (c) illustrates move-  
 93 ment between three social distancing classes, with subscripts 0, 1 and 2 denoting no social distancing,  
 94 some social distancing and complete isolation, respectively. Individuals can move up and down the so-  
 95 cial distancing ladder. Note that the disease progression pathway shown in Panel A is the same for all

96 individuals in different social distancing states (faded colours in Panel (a)). Movement between social  
 97 distancing classes is allowed unless infection status is known (and requires full social distancing for all  
 98 reported infections). Note that all infections transition from a susceptible state through to recovery but  
 99 with rates and probabilities dependent on the immunity and social distancing status. As such, we denote  
 100 our variables  $X_i^\xi$  where  $X \in \{S, E, P, I_S, I_A, R_S, R_A\}$  is the disease state, the subscript  $i \in \{0, 1, 2\}$   
 101 is the physical distancing level, and the superscript  $\xi \in \{u, v, w\}$  indicates immunity status. The  $M$   
 102 subscript in panel (a) indicates those who have tested positive for the virus and are thus isolated from the  
 103 population until recovery. We summarize each of the model disease classes as follows:

- 104 • Susceptible individuals denoted by  $(S(t)_i^\xi)$ , who are eligible to be infected by the pathogen.
- 105 • Exposed individuals denoted by  $(E(t)_i^\xi)$ , who have been infected but are incubating the virus.  
 106 They are not transmissible and have a low enough viral load that they would not test positive for  
 107 COVID-19.
- 108 • Pre-symptomatic individuals denoted by  $(P(t)_i^\xi)$ , who are infectious but have not had the disease  
 109 long enough to show symptoms.
- 110 • Infected-symptomatic individuals denoted by  $(I_S(t)_i^\xi)$  who are infectious and have started show-  
 111 ing symptoms.
- 112 • Infected-asymptomatic individuals denoted by  $(I_A(t)_i^\xi)$ , who are infectious and never show symp-  
 113 toms.
- 114 • Removed-symptomatic individuals denoted by  $(R_S(t)_i^\xi)$ , who were symptomatic, but are no  
 115 longer infectious.
- 116 • Removed-symptomatic individuals denoted by  $(R_A(t)_i^\xi)$ , who were asymptomatic, but are no  
 117 longer infectious,

118 with  $t$  as time in days since the onset of the pandemic, taken here to be March 10, 2020. For each of  
 119 the population classes, we consider three levels of physical distancing: no isolation (subscript 0), partial  
 120 isolation at contact reduction  $\delta$  (subscript 1) and full isolation (subscript 2). All compartments sum to  
 121 the total population,  $N$ , which is constant in time as we do not consider recruitment from birth or death.  
 122 The governing differential equations for the full model depicted in Figure 1 are detailed in the Appendix.

Table 1: The table shows what type of immunity each compartment has with  $\mathcal{N}^\xi = [S^\xi, E^\xi, P^\xi, P_M^\xi, I_S^\xi, I_{S_M}^\xi, I_A^\xi, I_{A_M}^\xi]$  and  $\mathcal{R}^\xi = [R_S^\xi, R_A^\xi, R_{S_M}^\xi, R_{A_M}^\xi]$ , where  $\xi \in \{u, v, w\}$ .

| Classes         | No immunity | Infection induced immunity | Vaccine induced immunity | Perceived induced immunity |
|-----------------|-------------|----------------------------|--------------------------|----------------------------|
| $\mathcal{N}^u$ | ✓           |                            |                          |                            |
| $\mathcal{R}^u$ |             | ✓                          |                          |                            |
| $\mathcal{N}^v$ |             |                            | ✓                        | ✓                          |
| $\mathcal{R}^v$ |             | ✓                          | ✓                        | ✓                          |
| $\mathcal{N}^w$ | ✓           |                            |                          | ✓                          |
| $\mathcal{R}^w$ |             | ✓                          |                          | ✓                          |

## 123 2.2 COVID-19 Testing

124 In this study, we compare the number of cumulative and active reported infections, seroprevalence, daily  
125 incidence, and positivity rate calculated by our model with the data provided by Public Health Ontario.

### 126 Active reported infections

127 Active reported infections,  $M_A$  are defined by the sum of reported pre-symptomatic, asymptomatic, and  
128 symptomatic cases with different immunity levels who have not yet recovered, i.e. would not yield a  
129 negative test result. We define them as

$$130 \quad M_A = \sum_{\substack{\xi \in \{u,v,w\} \\ i \in \{0,1,2\}}} \left( P_{M_i}^\xi + I_{S_{M_i}}^\xi + I_{A_{M_i}}^\xi \right). \quad (1)$$

131 Note that we assume that all reported infections will fully isolate.

### 132 Cumulative reported infections

133 We define  $M$  to be the cumulative newly reported cases. We define the rate of change of cumulative  
134 reported incidence as a sum of pre-symptomatic, asymptomatic, and symptomatic infections who have  
135 tested positive at time  $t$  as follows

$$136 \quad \dot{M} = \sum_{\substack{\xi \in \{u,v,w\} \\ i \in \{0,1,2\}}} \left( \rho_s^\xi I_{S_i}^\xi + \rho_a^\xi (P_i^\xi + I_{A_i}^\xi) \right). \quad (2)$$

### 137 Total Vaccination Administered

138 Cumulative Vaccination,  $V_A$  is the total vaccines administered. The rate of change here is defined by the  
139 sum of all eligible vaccine recipients who vaccinate at time  $t$  with rate  $p$  and is defined as

$$140 \quad \dot{V}_A = \sum_{i=0}^2 p \left( S_i^u + E_i^u + P_i^u + I_{A_i}^u + R_{A_i}^u \right). \quad (3)$$

141 Importantly we assume that those who have symptomatic infection, have recovered from symptomatic  
142 infection, or have tested positive for having an infection are ineligible to receive a vaccine.

### 143 Seroprevalence

144 Serology testing, which tests someone's blood to see if they have antibodies for COVID-19, is used as  
145 a measure of population-level infection and immunity. Seroprevalence,  $S_R$  is estimated by the number  
146 of people who test positive for COVID-19 antibodies based on serology data. Herein, we assume that  
147 people with COVID-19 antibodies will belong to the recovered class and thus

$$148 \quad S_R = \sum_{\substack{\xi \in \{u,v,w\} \\ i \in \{0,1,2\}}} \left( R_{S_i}^\xi + R_{A_i}^\xi + R_{S_{M_i}}^\xi + R_{S_{A_i}}^\xi \right). \quad (4)$$

149 We note that individuals that wane out of the recovered classes will not have positive serology tests in  
150 our model.

### 151 **Daily Reported Infection Incidence**

152  $D_I$  refers to the number of newly diagnosed COVID-19 cases per day, and is defined as

$$153 \quad D_I = M(t) - M(t - 1). \quad (5)$$

### 154 **Positivity Rate**

Since we assume that all individuals are eligible for testing then we can define the test positivity rate as the number of positive tests (daily incidence) divided by total tests administered across the entire population. We define the testing rate of symptomatic infections to be  $\rho_s$ , and assume that the testing rate for all populations that are not infected or that have asymptomatic infection to have testing rate  $\rho_a$ . Thus, we define the total tests  $T_T$

$$T_T = \sum_{\substack{\xi \in \{u,v,w\} \\ i \in \{0,1,2\}}} \left[ \rho_a^\xi \left( S_i^\xi(t) + E_i^\xi(t) + P_i^\xi(t) + I_{A_i}^\xi(t) + R_{S_i}^\xi(t) + R_{A_i}^\xi(t) \right) + \rho_s^\xi I_{S_i}^\xi \right]$$

and the test positivity rate

$$\rho^+ := \frac{D_I}{T_T}.$$

### 155 **2.3 Physical distancing functions**

156 We model the transition between the different social distancing classes as in [20], by assuming that  
157 individuals who are not vaccinated move from social distancing class 0 to class 1 with rate  $\mu^u$  given by

$$158 \quad \mu^u = \mu_{\max} \left( \frac{[K_M - K_c]_+}{[K_M - K_c]_+ + K_0 - K_c} \right) \left( \frac{[M_A - M_c]_+}{[M_A - M_c]_+ + M_0 - M_c} \right), \quad (6)$$

where  $\mu_{\max}$  is the maximal rate of social distancing,  $[\cdot]_+ = \max(\cdot, 0)$ , and  $K_M$  is the doubling rate given by

$$K_M = \frac{dM/dt}{M \ln(2)}.$$

159 We assume that individuals transition from social distancing class 1 to class 2 with rate  $\mu^u/2$  to take  
160 into account that people who have already reduced their contacts will be slower in fully isolating. Fur-  
161 thermore, we assume that individuals who are vaccinated are also slower in transitioning from social  
162 distancing class 0 to 1 by setting  $\mu^v = \mu^w = \mu^u/2$ . As we can see from the definition of the physical  
163 distancing function  $\mu$ , the number of total and active reported cases determine if individuals will physical  
164 distance, and these two quantities are provided from testing.

165 Additionally, individuals decrease social distancing based on some cost,  $C$ , with rate  $\nu$  defined as  
 166 in [20],

$$167 \quad \nu = \nu_{\max} \left( \frac{[C - C_c]_+}{[C - C_c]_+ + C_0 - C_c} \right), \quad (7)$$

where  $\nu_{\max}$  is the maximal rate at which physical distancing can be relaxed. The cost of social distancing, primarily introduced by [20], is extended as follows

$$\dot{C} = \frac{N_{crit}}{N} \sum_{\xi \in \{u, v, w\}} ((S_2^\xi + E_2^\xi) + (1 - \delta)(S_1^\xi + E_1^\xi)), \quad (8)$$

168 where the full cost occurs to those in all immunity groups who are susceptible or exposed (i.e. would test  
 169 positive for the virus). As was done by Moyles et al. in [20], the cost is scaled to be in days where one  
 170 day represents the cost of the entire population,  $N$ , fully or partially isolating. Individuals in the social  
 171 distance class 1 have reduced transmissibility by a factor  $\delta$ , and we assume this comes at a reciprocal  
 172 burden cost of  $(1 - \delta)$  per day.

## 173 2.4 Parameter Values and Estimation

174 In this study we estimate parameters (i)  $K_c$ : critical approximate disease doubling rate to induce social  
 175 distancing, (ii)  $M_c$ : critical active cases to induce social distancing, and (iii)  $\rho_a$ : testing rate for asymp-  
 176 tomatic person to test positive as these parameters are assumed to vary within different public health  
 177 mitigation periods. Additionally, we estimate  $p$ , the percentage of vaccinated people. We estimate these  
 178 parameters in different time windows defined by the time period over which certain policies were in ef-  
 179 fect to investigate how their values change based on NPIs and pharmaceutical interventions. We choose  
 180 the date and the category of the implemented NPI as developed by Dick et al. [38] where the authors  
 181 used government resources and creditable news agencies to provide the timeline of categorized public  
 182 health interventions from March 12, 2020, to January 5, 2022. In Table 2, we provide the dates of each  
 183 time window and the corresponding policy.

184 For parameter fitting we use data from Public Health Ontario [36, 37] on cumulative and active  
 185 reported cases, and total vaccines administered from March 10, 2020 to November 30, 2021. We start  
 186 with an initial value for the first time window for the values of the parameters  $K_c$ ,  $M_c$ ,  $\rho_a$  and  $p$ , and  
 187 then employ a non-linear least squares method to find the values of the parameters so that the simulated  
 188 cumulative and active reported cases, and total number of vaccinations, best fit the data. For the second  
 189 time window we use as initial value of the fitted values from the first time window, and estimate the  
 190 values of the parameters again using the same fitting method. We repeat the same procedure until we  
 191 have estimated the values of the parameters for all time windows.

192 The remaining model parameters are assigned the values listed in Tables 2 and in the Appendix.

## 193 2.5 Initial Conditions

194 We initialize all compartments to be zero except for the symptomatic infectious  $I_S^0$  and the susceptible  
 195  $S^0$ , assuming that  $I_S^0(t = 0) = 0.002N/N_{crit}$  and  $S^0(t = 0) = 0.98N/N_{crit}$ , where  $t = 0$  is the initial  
 196 time and  $N_{crit}$  is the critical population at which healthcare resources are overwhelmed.



Table 2: Estimated values of  $K_c$ ,  $M_c$ ,  $\rho$  and  $p$ .

| Time window | Important dates |             | Rationale                        | $\beta$    | $K_c$  | $M_c$  | $\rho_a$ | $p$    |
|-------------|-----------------|-------------|----------------------------------|------------|--------|--------|----------|--------|
| 1           | 10-Mar-2020     | 07-Jun-2020 | Lockdown and gradual reopening   | -          | 0.0635 | 0.0239 | 0.0094   | -      |
| 2           | 07-Jun-2020     | 20-Aug-2020 | Stage 2 and 3 mosaic             | -          | 0.0635 | 0.0239 | 0.0061   | -      |
| 3           | 20-Aug-2020     | 25-Dec-2020 | Tightening Measures, second wave | -          | 0.0160 | 0.0000 | 0.0021   | -      |
| 4           | 25-Dec-2020     | 19-Jan-2021 | Tightening Measures, second wave | -          | 0.0000 | 0.2885 | 0.0024   | -      |
| 5           | 19-Jan-2021     | 28-Jan-2021 | Stay at home                     | -          | 0.0000 | 0.0000 | 0.0024   | -      |
| 6           | 28-Jan-2021     | 15-Feb-2021 | Stay at home                     | -          | 0.0031 | 0.0000 | 0.0038   | -      |
| 7           | 15-Feb-2021     | 12-Mar-2021 | Reopening scenarios              | $1.5\beta$ | 0.0048 | 0.0000 | 0.0040   | 0.0011 |
| 8           | 12-Mar-2021     | 04-Apr-2021 | Reopening scenarios              | $1.5\beta$ | 0.0070 | 0.0000 | 0.0020   | 0.0000 |
| 9           | 04-Apr-2021     | 09-May-2021 | Emergency stay at home           | $1.5\beta$ | 0.0000 | 0.3312 | 0.0024   | 0.0002 |
| 10          | 09-May-2021     | 10-Jun-2021 | Emergency stay at home           | $1.5\beta$ | 0.0000 | 0.0000 | 0.0029   | 0.0016 |
| 11          | 10-Jun-2021     | 15-Jun-2021 | S1                               | $1.5\beta$ | 0.0096 | 0.0097 | 0.0040   | 0.0187 |
| 12          | 15-Jun-2021     | 29-Jun-2021 | S1                               | $1.5\beta$ | 0.0096 | 0.0097 | 0.0043   | 0.0153 |
| 13          | 29-Jun-2021     | 15-Jul-2021 | S2                               | $2\beta$   | 0.0096 | 0.0097 | 0.0010   | 0.0288 |
| 14          | 15-Jul-2021     | 01-Sep-2021 | S3                               | $2\beta$   | 0.0096 | 0.0097 | 0.0003   | 0.0221 |
| 15          | 01-Sep-2021     | 30-Nov-2021 | S3                               | $2\beta$   | 0.0096 | 0.0097 | 0.0020   | 0.0230 |

## 197 2.6 Sensitivity Analysis

198 We perform a sensitivity analysis on the waning parameters  $\omega_I, \omega_V, \omega_W$  and the vaccine efficacy  $\epsilon$ .  
 199 To do so we generate 1000 samples of the parameters  $\epsilon, \omega_I, \omega_V$ , and  $\omega_W$  using the Latin hypercube  
 200 method [40]. We assumed that the quickest vaccine induced immunity  $\omega_V$  or infection induced immunity  
 201  $\omega_I$ , can wane is 4 months, and the slowest is 2 years [35]. The quickest the perceived induced immunity  
 202  $\omega_W$  can wane is 4 months, and the slowest is 1 years [41]. We did not test the sensitivity of our model  
 203 on the other parameters since our model is an extension of the model presented in [20] and the authors  
 204 carried out sensitivity analysis on the model parameters. However, the waning parameters  $\omega_I, \omega_V$ , and  
 205  $\omega_W$  and the vaccine efficacy  $\epsilon$  are new parameters.

206 We take into account that the emergence of SARS-CoV-2 variants can affect transmission rate of  
 207 the disease. If we define  $\beta$  as the transmission coefficient for the wild-type strain then when the Alpha  
 208 variant (B.1.1.17) was dominant between February 15 and June 29, 2021 we modify the transmission  
 209 coefficient to  $1.5\beta$  accounting for the higher reproduction number of this variant [42]. Similarly, from  
 210 June 29, 2021 to December 31, 2021 the Delta variant (B.1.617.2) was dominant and we modify the  
 211 transmission to  $2\beta$  [42]. For a subset of parameters, reasonable values were specified based on Health  
 212 statistics, see Table 1 and 3 in the Appendix.

## 213 3 Results

### 214 3.1 Time windows

215 We provide the fitting results for each time window in Table 2. From the start of the pandemic until  
 216 August 20, 2020 (time windows 1 and 2), the values of the parameters  $K_c$  and  $M_c$  remain the same



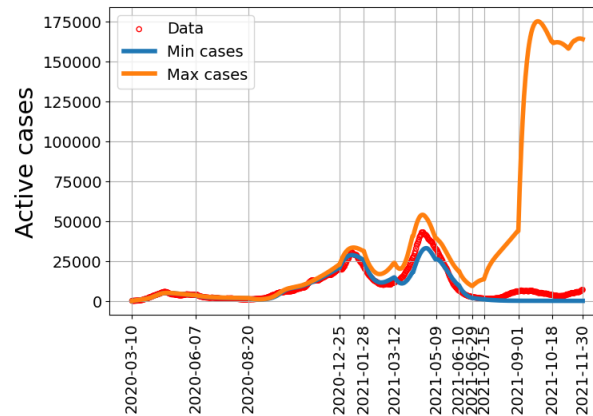


Figure 2: The minimum and maximum number of active cases per day, obtained by numerically solving the model equations, for different values of  $\epsilon$ ,  $\omega_I$ ,  $\omega_V$  and  $\omega_W$ .

217 indicating that individuals had the same level of vigilance during that time period, while the testing  
 218 rate  $\rho_a$  is high during the first time window, but it decreases during the second time window. The  
 219 decrease in the values of  $K_c$  and  $M_c$  between August 20 and December 25, 2020 shows that individuals  
 220 became more cautious, while testing decreases further compared to the previous time period. During  
 221 that time window, more strict measures were implemented in Ontario explaining the increased vigilance.  
 222 During time window 4, we observe that the value of  $K_c$  drops, but the values of  $M_c$  and  $\rho_a$  increase.  
 223 Increase in the value of  $M_c$  indicates that more cases are needed to induce social distancing, but the  
 224 critical doubling rate is zero meaning that any increase in the doubling rate leads to more vigilance.  
 225 Increase in the value of  $M_c$  and reduction in the value of  $K_c$  might occur during the exponential phase  
 226 of spread of the disease when the number of cases might not be high, but the doubling rate is high and  
 227 individuals are more cautious knowing that the number of cases is exponentially growing. From January  
 228 19 to February 15, 2021 (time windows 5 and 6), a stay-at-home order was in effect in Ontario, and  
 229 this resulted in people increasing social distancing as the value of  $M_c$  remains zero implying that any  
 230 number of cases triggers social distancing. From February 15 to April 4, 2021 (time windows 7 and  
 231 8), although the government was considering relaxation of the mitigation measures, the values of  $M_c$   
 232 remain zero showing that individuals were still vigilant and continue to social distance if the number of  
 233 cases is non-zero. During time windows 9 and 10, the stay-at-home order was again in effect. Although,  
 234 the value of  $M_c$  increased during time window 9, the value of  $K_c$  remains zero for both time windows  
 235 indicating that people are reducing their contacts if the doubling rate is greater than zero. Finally, from  
 236 June 10 to November 30, 2021 (time windows 11 to 15), the values of  $K_c$  and  $M_c$  remain constant and  
 237 increase compared to the time period between May 9 and June 15. It is possible that the increase in  
 238 vaccine coverage resulted in people being more relaxed about social distancing, and would reduce their  
 239 social activities only when the doubling rate or number of cases would surpass the value of  $K_c$  and  $M_c$ ,  
 240 respectively.

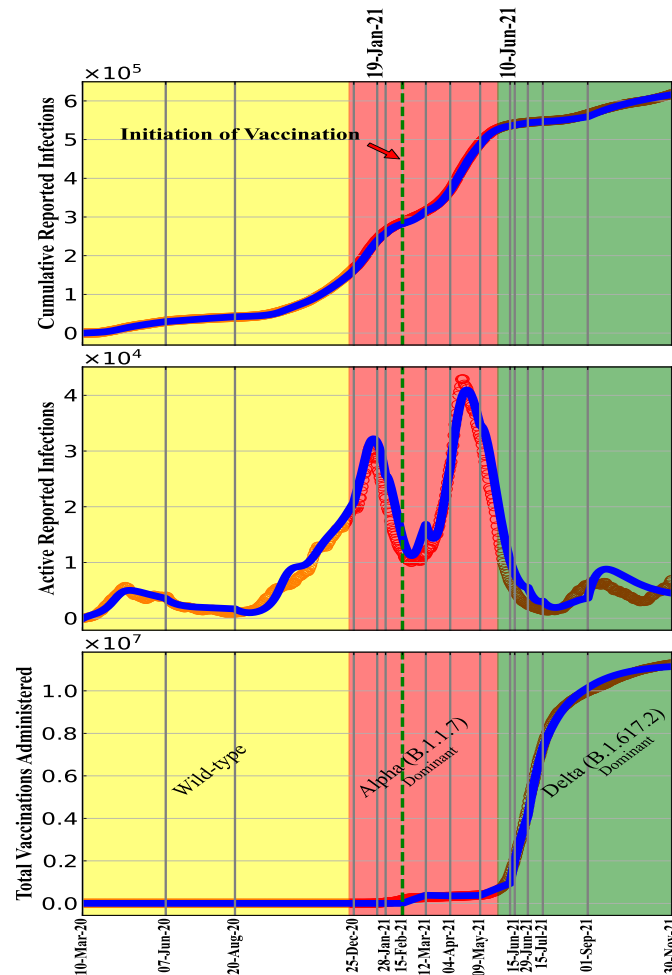


Figure 3: Comparison between model simulations and Ontario Data Catalogue. Model predictions fits to data from [36] in panel (a) and (b), and fits to data from [37] in panel (c), from March 10 2020 to November 30 2021. The green vertical dashed line shows the vaccination starting date. In the red (green) shade area the diseases transmission rate of the variants, was assumed to be one and half times (double) greater than the transmission rate of wild type.

### 241 3.2 Waning immunity

242 In Figure 2 we present the results from our sensitivity analysis on the daily minimum and maximum  
 243 active cases given by the 1000 samples of the parameters  $\epsilon, \omega_I, \omega_V, \omega_W$  and the estimated values of  
 244  $K_c, M_c, \rho$  and  $p$ . The values for  $\omega_I$  and  $\omega_V$  are chosen on a per-day basis, and We observe that the  
 245 minimum and maximum number of daily active cases are similar in magnitude up to December 25,  
 246 2020, which implies that model predictions are not affected by the waning immunity parameters up to  
 247 this date. The minimum number of cases (blue line) corresponds to values of the parameters  $\omega_I$  between  
 248 0.0013 and 0.0016, and  $\omega_V$  between 0.0015 and 0.0020, (both very close to the assumed two-year upper  
 249 bound) we can see that the model predicts no infection after July 29, 2021. . This shows that if we

250 assume slow waning rates, the model does not capture the fourth wave, meaning that the number of  
 251 individuals left in the susceptible compartment is not sufficiently large for the disease to spread. On the  
 252 other hand, the model overestimates the number of active cases after July 29, 2021, if we assume that  
 253 the infection and vaccine induced immunity fade quickly (red line) with  $\omega_V \in (0.0075, 0.0082)$  and  
 254  $\omega_I \in (0.0062, 0.0074)$  near the assumed 4-month lower bound in waning time.

### 255 3.3 Model Prediction Vs. Observed Data

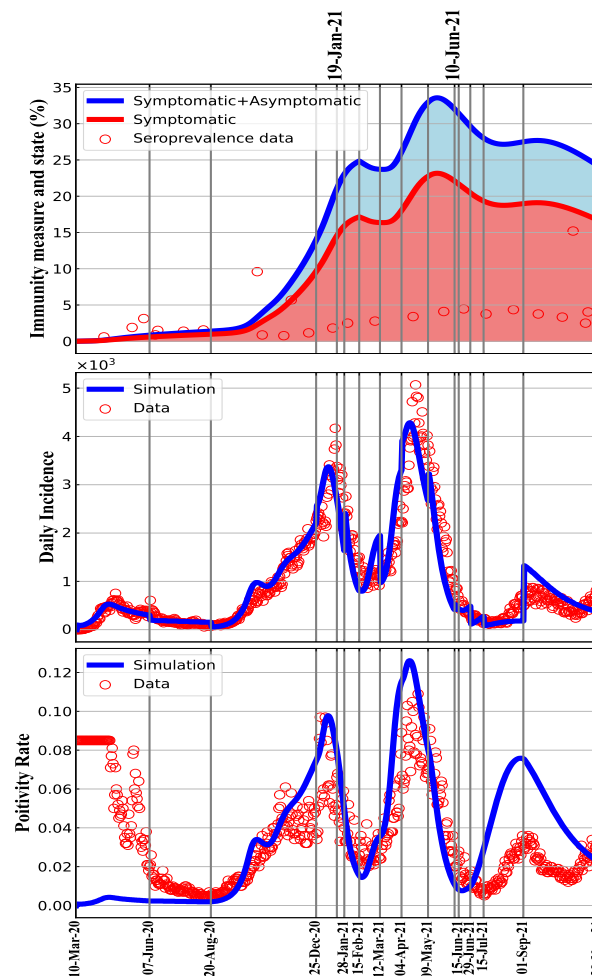


Figure 4: The simulation results for the seroprevalence, daily incidence and positivity rate have been projected with health data from March 10 2020 to November 30, 2021.

256 The results from the model fitting of  $K_c$ ,  $M_c$ ,  $\rho_a$  and  $p$  are illustrated in Figure 3. Here, we also  
 257 plot data on cumulative reported infections (top panel), active reported infections (middle panel), and the  
 258 total vaccines administered (bottom panel) [37]. We observe a satisfactory model prediction of observed  
 259 data for cumulative incidence and total vaccination administered criteria between March 10, 2022, and

260 November 30, 2021. For active reported infections, the fit is satisfactory until August 2021 after which  
261 there is an overshoot compared to the data.

262 Further, we compare the model results with data which was not used to fit the model, particularly  
263 seroprevalence, daily incidence, and positivity rate. The evolution of model predicted seroprevalence  
264 in different cohorts, daily incidence, positivity rate, and the corresponding health data are depicted over  
265 time in Figure 4. Although, there is a relatively good agreement between data and simulation for daily  
266 incidence and positivity rate, the estimated seroprevalence is higher than the data suggest. The data  
267 on seroprevalence are based on studies from blood donors aged 16+ from Canadian Blood Services  
268 (CBS) [39, 43]. We note here that our model does not distinguish between serology and T-cell medi-  
269 ated immunity whereas the CBS data report the results from serological testing only. It is possible for  
270 individuals to have T-cell immunity even when antibody levels have waned. A recent study reported  
271 that high T-cell memory levels can protect against COVID-19 infection [44]. Additionally, we assume a  
272 well-mixed population in our model. This can also increase our estimates as we do not include contact  
273 networks. Finally, our model presents immunity from the entire population irrespective of age whereas  
274 the CBS serological testing is conducted in ages 16+ only. The inclusion of age structure and con-  
275 tact matrices may reduce our seroprevalence estimates. However, even with age-structuring Dick et al.  
276 estimated seroprevalence higher than suggested by the data, although less of a difference than we see  
277 here [35] Given these points we find that it is not surprising that our model and the data do not agree. In  
278 future, we will consider a model with age-structure to see if this will provide immunity estimates closer  
279 to the serological testing data.

280

## 281 **4 Discussion**

282 In this work, we proposed a compartmental model coupling the effects of dynamic social distancing and  
283 cost-based relaxation, different immunity levels, vaccination, and new variants of concern to study which  
284 can recreate the history of the COVID-19 pandemic up to December 2021 in Ontario. The model can  
285 predict different quantities of interest including active cases, vaccination, daily incidence and positivity  
286 rate. However, our model predictions on the seroprevalence are different from the data which could  
287 be due to the challenges on estimating population seroprevalence from serological testing and/or the  
288 homogeneous mixing assumption for our model.

289 We concluded that if we assume that it takes 2 years for disease or vaccine induced immunity to wane,  
290 our model does not capture the fourth wave in Ontario. Our sensitivity analysis showed that waning  
291 immunity would not change anything in the model predictions on active cases until December 25, 2020.  
292 However, the model is more sensitive after December 25, 2020, and the values of the waning parameters  
293 affect the fitting results. Our simulations and sensitivity analysis showed that waning immunity is crucial  
294 to capture more accurately the disease dynamics and predict multiple waves over a long time period. In  
295 future work, we want to extend the time period to include the Omicron variant and study the effect of  
296 evading immunity on disease dynamics.

297 We estimated key parameters affecting the vigilance of individuals at different time windows and  
298 found that NPIs influence how they increase or decrease their contacts. For example, they are more  
299 cautious when stricter measures are introduced such as stay-at-home orders or lockdowns. Our results  
300 also indicate that people started being more relaxed about social distancing after May 2021, which is

301 approximately when vaccine coverage increased in Canada. This shows the importance of having a  
302 model that incorporates dynamic human behaviour in order to capture how people change their behaviour  
303 based on the disease dynamics and NPIs.

304 As a case study, we used different health data from Ontario to evaluate our model predictions. How-  
305 ever, our modeling framework can be easily adapted to any other country or province for which relevant  
306 data are available. Our modelling approach can provide important insights how NPIs and vaccination  
307 can influence the health decisions people make during epidemics, and better understand how disease  
308 dynamics are affected by those decisions.

## 309 **CRediT authorship contribution statement**

310 **Jeta Molla:** Conceptualization, Methodology, Software, Visualization, Writing – original draft, Writing  
311 – review & editing. **Suzan Farhang-Sardroodi:** Conceptualization, Methodology, Software, Visualiza-  
312 tion, Data Curation, Investigation. **Iain R Moyles:** Conceptualization, Methodology, Software, Funding  
313 acquisition, Supervision, Writing – original draft, Writing – review & editing. **Jane M Heffernan:**  
314 Conceptualization, Methodology, Funding acquisition, Supervision, Writing – review & editing.

## 315 **Acknowledgments**

316 This work was supported by NSERC (JMH, IM), CIHR (JMH), and the OMNI-REUNI NSERC-PHAC  
317 Emerging Infectious Disease Modelling Initiative (JMH, IM). JM would like to acknowledge support  
318 from an OMNI-REUNI postdoctoral fellowship.

## 319 **References**

- 320 [1] Amelie Desvars-Larrive, Elma Dervic, Nina Haug, Thomas Niederkrotenthaler, Jiaying Chen,  
321 Anna Di Natale, Jana Lasser, Diana S Gliga, Alexandra Roux, Johannes Sorger, et al. A struc-  
322 tured open dataset of government interventions in response to covid-19. *Scientific data*, 7(1):1–9,  
323 2020.
- 324 [2] Nils Haug, Lukas Geyrhofer, Alessandro Londei, Elma Hot Dervic, Amélie Desvars, Vittorio  
325 Loreto, Beate Conrady, Stefan Thurner, and Peter Klimek. Ranking the effectiveness of world-  
326 wide covid-19 government interventions. *Nature Human Behaviour*, 4:1303–1312, July 2020.
- 327 [3] Nicola Perrà. Non-pharmaceutical interventions during the covid-19 pandemic: A review. *Physics*  
328 *Reports*, 913:1–52, 2021.
- 329 [4] Oliver J Watson, Gregory Barnsley, Jaspreet Toor, Alexandra B Hogan, Peter Winskill, and Azra C  
330 Ghani. Global impact of the first year of covid-19 vaccination: a mathematical modelling study.  
331 *The Lancet Infectious Diseases*, 22(9):1293–1302, 2022.
- 332 [5] Constantino Caetano, Maria Luísa Morgado, Paula Patrício, Andreia Leite, Ausenda Machado,  
333 André Torres, João Freitas Pereira, Sónia Namorado, Ana Sottomayor, André Peralta, and Baltazar

- 334 Nunes. Measuring the impact of covid-19 vaccination and immunity waning: A modelling study  
335 for portugal. Vaccine, 40(49):7115–7121, 2022.
- 336 [6] Carolina Ribeiro Xavier, Rafael Sachetto Oliveira, Vinícius da Fonseca Vieira, Bernardo Mar-  
337 tins Rocha, Ruy Freitas Reis, Bárbara de Melo Quintela, Marcelo Lobosco, and Rodrigo Weber  
338 Dos Santos. Timing the race of vaccination, new variants, and relaxing restrictions during covid-19  
339 pandemic. Journal of Computational Science, 61:101660, 2022.
- 340 [7] Sheila F Lumley, Gillian Rodger, Bede Constantinides, Nicholas Sanderson, Kevin K Chau,  
341 Teresa L Street, Denise O’Donnell, Alison Howarth, Stephanie B Hatch, Brian D Marsden, Stu-  
342 art Cox, Tim James, Fiona Warren, Liam J Peck, Thomas G Ritter, Zoe de Toledo, Laura Warren,  
343 David Axten, Richard J Cornall, E Yvonne Jones, David I Stuart, Gavin Screatton, Daniel Ebner,  
344 Sarah Hoosdally, Meera Chand, Derrick W Crook, Anne-Marie O’Donnell, Christopher P Conlon,  
345 Koen B Pouwels, A Sarah Walker, Tim E A Peto, Susan Hopkins, Timothy M Walker, Nicole E  
346 Stoesser, Philippa C Matthews, Katie Jeffery, David W Eyre, and Oxford University Hospitals  
347 Staff Testing Group. An Observational Cohort Study on the Incidence of Severe Acute Respira-  
348 tory Syndrome Coronavirus 2 (SARS-CoV-2) Infection and B.1.1.7 Variant Infection in Healthcare  
349 Workers by Antibody and Vaccination Status. Clinical Infectious Diseases, 74(7):1208–1219, 07  
350 2021.
- 351 [8] Lauren Childs, David W Dick, Zhilan Feng, Jane M Heffernan, Jing Li, and Gergely Röst. Model-  
352 ing waning and boosting of covid-19 in canada with vaccination. Epidemics, page 100583, 2022.
- 353 [9] Piero Poletti, Marco Ajelli, and Stefano Merler. The effect of risk perception on the 2009 h1n1  
354 pandemic influenza dynamics. PloS one, 6(2):e16460, 2011.
- 355 [10] Neil Ferguson. Capturing human behaviour. Nature, 446(7137):733–733, 2007.
- 356 [11] Raffaele Vardavas, Pedro Nascimento de Lima, Paul K Davis, Andrew M Parker, and Lawrence  
357 Baker. Modeling infectious behaviors: The need to account for behavioral adaptation in covid-19  
358 models. Journal on Policy and Complex Systems• Volume, 7(1), 2021.
- 359 [12] Priyanka Harjule, Vinita Tiwari, and Anupam Kumar. Mathematical models to predict covid-19  
360 outbreak: An interim review. Journal of Interdisciplinary Mathematics, 24(2):259–284, 2021.
- 361 [13] Aniruddha Adiga, Devdatt Dubhashi, Bryan Lewis, Madhav Marathe, Srinivasan Venkatramanan,  
362 and Anil Vullikanti. Mathematical models for covid-19 pandemic: a comparative analysis. Journal  
363 of the Indian Institute of Science, 100(4):793–807, 2020.
- 364 [14] Subramanian Shankar, Sourya Sourabh Mohakuda, Ankit Kumar, PS Nazneen, Arun Kumar Yadav,  
365 Kaushik Chatterjee, and Kaustuv Chatterjee. Systematic review of predictive mathematical models  
366 of covid-19 epidemic. Medical journal armed forces India, 77:S385–S392, 2021.
- 367 [15] William Ogilvy Kermack and Anderson G McKendrick. Contributions to the mathematical theory  
368 of epidemics. ii.—the problem of endemicity. Proceedings of the Royal Society of London. Series  
369 A, containing papers of a mathematical and physical character, 138(834):55–83, 1932.

- 370 [16] Juliana Tolles and ThaiBinh Luong. Modeling epidemics with compartmental models. Jama,  
371 323(24):2515–2516, 2020.
- 372 [17] Lingcai Kong, Mengwei Duan, Jin Shi, Jie Hong, Zhaorui Chang, and Zhijie Zhang. Compart-  
373 mental structures used in modeling covid-19: a scoping review. Infectious diseases of poverty,  
374 11(1):1–9, 2022.
- 375 [18] Piero Manfredi and Alberto D’Onofrio. Modeling the interplay between human behavior and the  
376 spread of infectious diseases. Springer Science & Business Media, 2013.
- 377 [19] Dale Weston, Katharina Hauck, and Richard Amlôt. Infection prevention behaviour and infectious  
378 disease modelling: a review of the literature and recommendations for the future. BMC public  
379 health, 18(1):1–16, 2018.
- 380 [20] Iain R Moyles, Jane M Heffernan, and Jude D Kong. Cost and social distancing dynamics in a  
381 mathematical model of covid-19 with application to ontario, canada. Royal Society open science,  
382 8(2):201770, 2021.
- 383 [21] Rebecca C Tyson, Noah D Marshall, and Bert O Baumgaertner. Transient prophylaxis and multiple  
384 epidemic waves. AIMS Mathematics, 7(4):5616–5633, 2022.
- 385 [22] Shi Zhao, Lewi Stone, Daozhou Gao, Salihu S Musa, Marc KC Chong, Daihai He, and Maggie H  
386 Wang. Imitation dynamics in the mitigation of the novel coronavirus disease (covid-19) outbreak  
387 in wuhan, china from 2019 to 2020. Annals of Translational Medicine, 8(7), 2020.
- 388 [23] Thomas Usherwood, Zachary LaJoie, and Vikas Srivastava. A model and predictions for covid-19  
389 considering population behavior and vaccination. Scientific Reports, 11(1):1–11, 2021.
- 390 [24] Zachary LaJoie, Thomas Usherwood, Shailen Sampath, and Vikas Srivastava. A covid-19 model  
391 incorporating variants, vaccination, waning immunity, and population behavior. Scientific Reports,  
392 12(1):1–11, 2022.
- 393 [25] Mohammadali Dashtbali and Mehdi Mirzaie. A compartmental model that predicts the effect of  
394 social distancing and vaccination on controlling covid-19. Scientific Reports, 11(1):1–11, 2021.
- 395 [26] Calistus N Ngonghala, Palak Goel, Daniel Kutor, and Samit Bhattacharyya. Human choice to self-  
396 isolate in the face of the covid-19 pandemic: a game dynamic modelling approach. Journal of  
397 Theoretical Biology, 521:110692, 2021.
- 398 [27] KM Ariful Kabir and Jun Tanimoto. Evolutionary game theory modelling to represent the be-  
399 havioural dynamics of economic shutdowns and shield immunity in the covid-19 pandemic. Royal  
400 Society open science, 7(9):201095, 2020.
- 401 [28] Kathryn R Fair, Vadim A Karatayev, Madhur Anand, and Chris T Bauch. Estimating covid-19 cases  
402 and deaths prevented by non-pharmaceutical interventions, and the impact of individual actions: A  
403 retrospective model-based analysis. Epidemics, 39:100557, 2022.



- 404 [29] Juan Pablo Gutiérrez-Jara, Katia Vogt-Geisse, Maritza Cabrera, Fernando Córdova-Lepe, and  
405 María Teresa Muñoz-Quezada. Effects of human mobility and behavior on disease transmission  
406 in a covid-19 mathematical model. Scientific Reports, 12(1):1–18, 2022.
- 407 [30] Carole Vignals, David W Dick, Rodolphe Thiébaud, Linda Wittkop, Mélanie Prague, and Jane M  
408 Heffernan. Barrier gesture relaxation during vaccination campaign in france: modelling impact of  
409 waning immunity. COVID, 1(2):472–488, 2021.
- 410 [31] M Alper Çenesiz and Luís Guimarães. Covid-19: What if immunity wanes? Canadian Journal of  
411 Economics/Revue canadienne d'économique, 55:626–664, 2022.
- 412 [32] Nursanti Anggriani, Meksianis Z Ndi, Rika Amelia, Wahyu Suryaningrat, and Mochammad And-  
413 hika Aji Pratama. A mathematical covid-19 model considering asymptomatic and symptomatic  
414 classes with waning immunity. Alexandria Engineering Journal, 61(1):113–124, 2022.
- 415 [33] Jennie S Lavine, Ottar N Bjornstad, and Rustom Antia. Immunological characteristics govern the  
416 transition of covid-19 to endemicity. Science, 371(6530):741–745, 2021.
- 417 [34] Chryssi Giannitsarou, Stephen Kissler, and Flavio Toxvaerd. Waning immunity and the second  
418 wave: Some projections for sars-cov-2. American Economic Review: Insights, 3(3):321–38, 2021.
- 419 [35] David W Dick, Lauren Childs, Zhilan Feng, Jing Li, Gergely Röst, David L Buckeridge, Nick H  
420 Ogden, and Jane M Heffernan. Covid-19 seroprevalence in canada modelling waning and boosting  
421 covid-19 immunity in canada a canadian immunization research network study. Vaccines, 10(1):17,  
422 2021.
- 423 [36] Public health ontario. 2020 covid-19 data. [https://data.ontario.ca/dataset/  
424 status-of-covid-19-cases-in-ontario](https://data.ontario.ca/dataset/status-of-covid-19-cases-in-ontario). Accessed: 2023-3-23.
- 425 [37] Public health ontario. 2020 covid-19 data. [https://data.ontario.ca/dataset/  
426 covid-19-vaccine-data-in-ontario](https://data.ontario.ca/dataset/covid-19-vaccine-data-in-ontario). Accessed: 2023-3-23.
- 427 [38] Covid-policy Canada. [https://github.com/ddick8/Covid-19-Policy-Response-Canadian-tracker/  
428 126](https://github.com/ddick8/Covid-19-Policy-Response-Canadian-tracker/) (2022).
- 429 [39] Seroprevalence in Canada. [https://www.covid19immunitytaskforce.ca/  
430 seroprevalence-in-canada/](https://www.covid19immunitytaskforce.ca/seroprevalence-in-canada/). Accessed: 2023-3-23.
- 431 [40] Wei-Liem Loh. On latin hypercube sampling. The annals of statistics, 24(5):2058–2080, 1996.
- 432 [41] Shannon Collinson and Jane M Heffernan. Modelling the effects of media during an influenza  
433 epidemic. BMC public health, 14(1):1–10, 2014.
- 434 [42] Diana Duong. Alpha, beta, delta, gamma: What's important to know about sars-cov-2 variants of  
435 concern?, 2021.
- 436 [43] CITEF. Task Force Funded Research; Technical Report. 2021. Available online:[https://www.  
437 covid19immunitytaskforce.ca/](https://www.covid19immunitytaskforce.ca/). Accessed: 2023-3-23.
- 438 [44] Paul Moss. The t cell immune response against sars-cov-2. Nature immunology, 23(2):186–193,  
439 2022.

## 440 Appendix

### 441 Sensitivity analysis

442 In Figure 5 we present the scatterplots for the estimated parameters  $K_c, M_c, \rho$  and  $p$  versus the waning  
443 rates  $\omega_I, \omega_V$ , and  $\omega_W$ . The results show that there is no relationship between  $K_c, M_c, \rho$  and  $\omega_I, \omega_V, \omega_W$ .  
444 The waning rates  $\omega_I, \omega_V$  and  $\omega_W$  determine how fast the infection or vaccine-induced immunity, and the  
445 perceived-induced immunity wane, and it would be expected that they do not influence the values of the  
446 behaviour parameters  $\rho, M_c, K_c$  since individuals do not know when their immunity wanes. While there  
447 is no relationship between  $p$  and  $\omega_I$ , the results indicate a negative relationship of moderate strength  
448 between  $p$  and  $\omega_V$ , and  $p$  and  $\omega_W$ . This implies that as the rate at which individuals transition from  $u$  to  
449  $w$  decreases, the vaccination rate has to increase to fit the vaccination data.

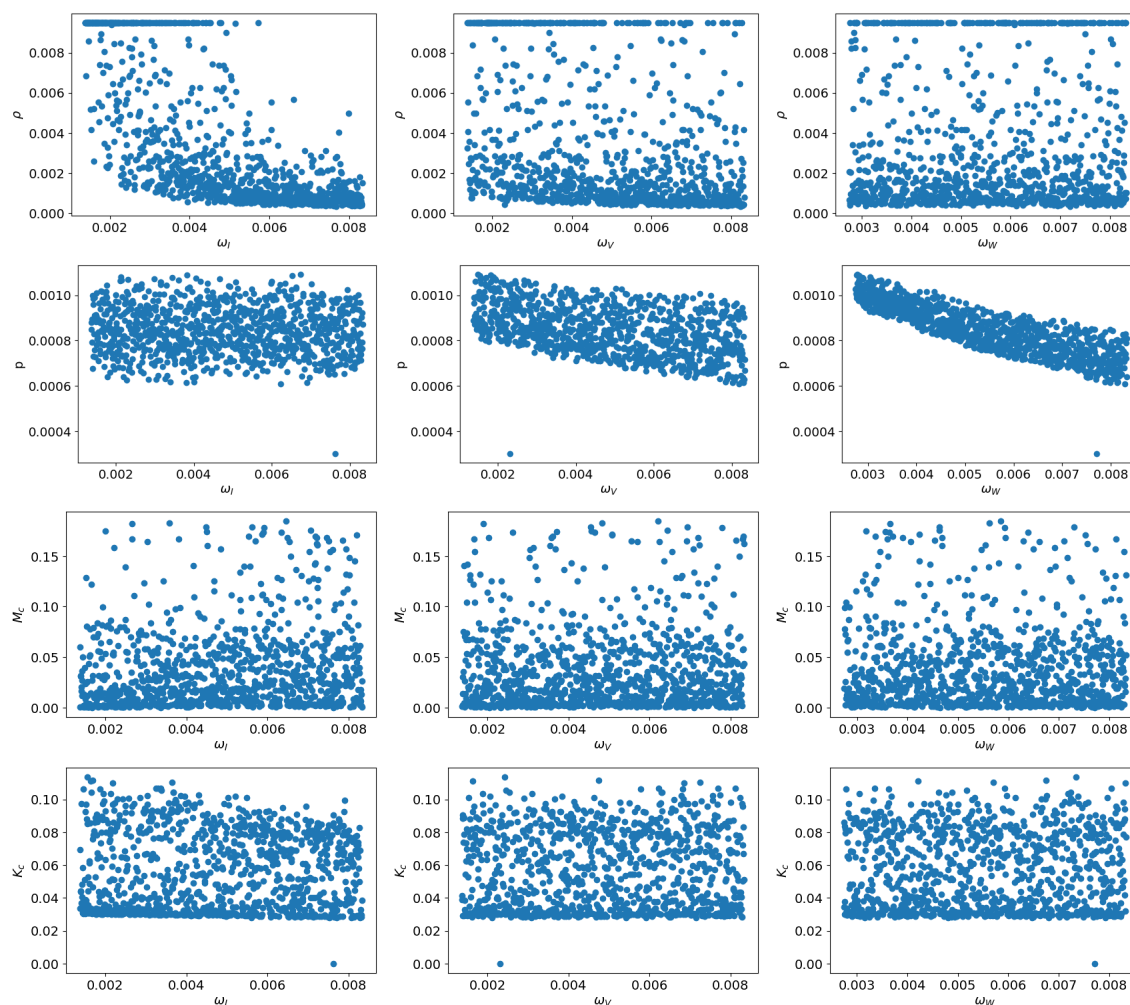


Figure 5: Scatterplots of the parameters  $K_c, M_c, \rho, p$  versus  $\omega_I, \omega_V$  and  $\omega_W$ .

## 450 Differential Equation Models

451 The differential equation models for people with natural immunity (Eq: A.9), vaccine/perceived induced  
 452 immunity (Eq: A.10) and perceived induced immunity (Eq: A.11) are given by the following equations.

### 453 4.1 Natural Immunity

$$\begin{aligned}
 \dot{S}_0^u &= -F_{S_0^u} - \mu S_0^u + (\nu/2)S_1^u + (1 - q_2)\nu S_2^u - pS_0^u + wS_0^w + w_I(R_{S_0^u}^u + R_{A_0^u}^u) \\
 \dot{S}_1^u &= -F_{S_1^u} - (\mu/2)S_1^u + q_1\mu S_0^u - (\nu/2)S_1^u + q_2\nu S_2^u - pS_1^u + wS_1^w + w_I(R_{S_1^u}^u + R_{A_1^u}^u) \\
 \dot{S}_2^u &= (1 - q_1)\mu S_0^u + (\mu/2)S_1^u - \nu S_2^u - pS_2^u + wS_2^w + w_I(R_{S_2^u}^u + R_{A_2^u}^u) \\
 \dot{E}_0^u &= F_{S_0^u} - \mu E_0^u + (\nu/2)E_1^u + (1 - q_2)\nu E_2^u - \sigma E_0^u - pE_0^u + wE_0^w \\
 \dot{E}_1^u &= F_{S_1^u} - (\mu/2)E_1^u + q_1\mu E_0^u - (\nu/2)E_1^u + q_2\nu E_2^u - \sigma E_1^u - pE_1^u + wE_1^w \\
 \dot{E}_2^u &= (1 - q_1)\mu E_0^u + (\mu/2)E_1^u - \nu E_2^u - \sigma E_2^u - pE_2^u + wE_2^w \\
 \dot{P}_0^u &= \sigma E_0^u - \mu P_0^u + (\nu/2)P_1^u + (1 - q_2)\nu P_2^u - \phi P_0^u - \rho_a P_0^u - pP_0^u + wP_0^w \\
 \dot{P}_1^u &= \sigma E_1^u - (\mu/2)P_1^u + q_1\mu P_0^u - (\nu/2)P_1^u + q_2\nu P_2^u - \phi P_1^u - \rho_a P_1^u - pP_1^u + wP_1^w \\
 \dot{P}_2^u &= \sigma E_2^u + (1 - q_1)\mu P_0^u + (\mu/2)P_1^u - \nu P_2^u - \phi P_2^u - \rho_a P_2^u - pP_2^u + wP_2^w \\
 \dot{P}_M^u &= \rho_a(P_0^u + P_1^u + P_2^u) - \phi P_M^u + wP_M^w \\
 \dot{I}_{S_0}^u &= q\phi P_0^u - \mu I_{S_0}^u - \gamma I_{S_0}^u - \rho_s I_{S_0}^u + wI_{S_0}^w \\
 \dot{I}_{S_1}^u &= q\phi P_1^u + q_I\mu I_{S_0}^u - \gamma I_{S_1}^u - \rho_s I_{S_1}^u + wI_{S_1}^w \\
 \dot{I}_{S_2}^u &= q\phi P_2^u + (1 - q_I)\mu I_{S_0}^u - \gamma I_{S_2}^u - \rho_s I_{S_2}^u + wI_{S_2}^w \\
 \dot{I}_{S_M}^u &= \rho_s(I_{S_0}^u + I_{S_1}^u + I_{S_2}^u) + q\phi P_M^u - \gamma I_{S_M}^u + wI_{S_M}^w \\
 \dot{I}_{A_0}^u &= (1 - q)\phi P_0^u - \mu I_{A_0}^u + (\nu/2)I_{A_1}^u + (1 - q_2)\nu_2 I_{A_2}^u - \gamma I_{A_0}^u - \rho_a I_{A_0}^u - pI_{A_0}^u + wI_{A_0}^w \\
 \dot{I}_{A_1}^u &= (1 - q)\phi P_1^u - (\mu/2)I_{A_1}^u + q_1\mu I_{A_0}^u - (\nu/2)I_{A_1}^u + q_2\nu I_{A_2}^u - \gamma I_{A_1}^u - \rho_a I_{A_1}^u - pI_{A_1}^u + wI_{A_1}^w \\
 \dot{I}_{A_2}^u &= (1 - q)\phi P_2^u + (1 - q_1)\mu I_{A_0}^u + (\mu/2)I_{A_1}^u - \nu I_{A_2}^u - \gamma I_{A_2}^u - \rho_a I_{A_2}^u - pI_{A_2}^u + wI_{A_2}^w \\
 \dot{I}_{A_M}^u &= \rho_a(I_{A_0}^u + I_{A_1}^u + I_{A_2}^u) + (1 - q)\phi P_M^u \gamma I_{A_M}^u + wI_{A_M}^w \\
 \dot{R}_{S_0}^u &= \gamma I_{S_0}^u - pR_{S_0}^u - w_I R_{S_0}^u + wR_{S_0}^w - \mu R_{S_0}^u + (\nu/2)R_{S_1}^u + \nu_2(1 - q_2)R_{S_2}^u \\
 \dot{R}_{S_1}^u &= \gamma I_{S_1}^u - pR_{S_1}^u - w_I R_{S_1}^u + wR_{S_1}^w + \mu q_1 R_{S_0}^u - (\mu/2)R_{S_1}^u - (\nu/2)R_{S_1}^u + \nu q_2 R_{S_2}^u \\
 \dot{R}_{S_2}^u &= \gamma I_{S_2}^u - pR_{S_2}^u - w_I R_{S_2}^u + wR_{S_2}^w + (\mu/2)R_{S_1}^u + \mu(1 - q_1)R_{S_0}^u - \nu R_{S_2}^u \\
 \dot{R}_{S_M}^u &= \gamma I_{S_M}^u - pR_{S_M}^u - w_I R_{S_M}^u + wR_{S_M}^w \\
 \dot{R}_{A_0}^u &= \gamma I_{A_0}^u - pR_{A_0}^u - w_I R_{A_0}^u + wR_{A_0}^w - \mu R_{A_0}^u + (\nu/2)R_{A_1}^u + \nu(1 - q_2)R_{A_2}^u \\
 \dot{R}_{A_1}^u &= \gamma I_{A_1}^u - pR_{A_1}^u - w_I R_{A_1}^u + wR_{A_1}^w + \mu q_1 R_{A_0}^u - (\mu/2)R_{A_1}^u - (\nu/2)R_{A_1}^u + \nu q_2 R_{A_2}^u \\
 \dot{R}_{A_2}^u &= \gamma I_{A_2}^u - pR_{A_2}^u - w_I R_{A_2}^u + wR_{A_2}^w + (\mu/2)R_{A_1}^u + \mu(1 - q_1)R_{A_0}^u - \nu R_{A_2}^u \\
 \dot{R}_{A_M}^u &= \gamma I_{A_M}^u - pR_{A_M}^u - w_I R_{A_M}^u + wR_{A_M}^w
 \end{aligned} \tag{A.9}$$

### 454 4.2 Vaccine/Perceived Induced Immunity

$$\dot{S}_0^v = -F_{S_0^v} - \mu S_0^v + (\nu/2)S_1^v + (1 - q_2)\nu S_2^v + q_v p S_0^u - w_I S_0^v$$

$$\begin{aligned}
\dot{S}_1^v &= -F_{S_1^v} - (\mu/2)S_1^v + q_1\mu S_0^v - (\nu/2)S_1^v + q_2\nu S_2^v + q_v p S_1^u - w'_I S_1^v \\
\dot{S}_2^v &= (1 - q_1)\mu S_0^v + (\mu/2)S_1^v - \nu S_2^v + q_v p S_2^u - w'_I S_2^v \\
\dot{E}_0^v &= F_{V_0} - \mu E_0^v + \nu E_1^v + (1 - q_2)\nu E_2^v - \sigma E_0^v + q_v p E_0^u \\
\dot{E}_1^v &= F_{V_1} - (\mu/2)E_1^v + q_1\mu E_0^v - (\nu/2)E_1^v + q_2\nu E_2^v - \sigma E_1^v + q_v p E_1^u \\
\dot{E}_2^v &= (1 - q_1)\mu E_0^v + (\mu/2)E_1^v - \nu E_2^v - \sigma E_2^v + q_v p E_2^u \\
\dot{P}_0^v &= \sigma E_0^v - \mu P_0^v + (\nu/2)P_1^v + (1 - q_2)\nu P_2^v - \phi P_0^v - \rho_a^v P_0^v + q_v p P_0^u \\
\dot{P}_1^v &= \sigma E_1^v - (\mu/2)P_1^v + q_1\mu P_0^v - (\nu/2)P_1^v + q_2\nu P_2^v - \phi P_1^v - \rho_a^v P_1^v + q_v p P_1^u \\
\dot{P}_2^v &= \sigma E_2^v + (1 - q_1)\mu P_0^v + (\mu/2)P_1^v - \nu P_2^v - \phi P_2^v - \rho_a^v P_2^v + q_v p P_2^u \\
\dot{P}_M^v &= \rho_a^v (P_0^v + P_1^v + P_2^v) - \phi P_M^v \\
\dot{I}_{S_0}^v &= q\phi P_0^v - \mu_I I_{S_0}^v - \gamma I_{S_0}^v - \rho_s^v I_{S_0}^v \\
\dot{I}_{S_1}^v &= q\phi P_1^v + q_I \mu_I I_{S_0}^v - \gamma I_{S_1}^v - \rho_s^v I_{S_1}^v \\
\dot{I}_{S_2}^v &= q\phi P_2^v + (1 - q_I)\mu_I I_{S_0}^v - \gamma I_{S_2}^v - \rho_s^v I_{S_2}^v \\
\dot{I}_{S_M}^v &= \rho_s^v (I_{S_0}^v + I_{S_1}^v + I_{S_2}^v) + q^v \phi P_M^v - \gamma I_{S_M}^v \\
\dot{I}_{A_0}^v &= (1 - q)\phi P_0^v - \mu I_{A_0}^v + (\nu/2)I_{A_1}^v + (1 - q_2)\nu I_{A_2}^v - \gamma I_{A_0}^v - \rho_a^v I_{A_0}^v + q_v p I_{A_0}^u \\
\dot{I}_{A_1}^v &= (1 - q)\phi P_1^v - (\mu/2)I_{A_1}^v + q_1\mu I_{A_0}^v - (\nu/2)I_{A_1}^v + q_2\nu I_{A_2}^v - \gamma I_{A_1}^v - \rho_a^v I_{A_1}^v + q_v p I_{A_1}^u \\
\dot{I}_{A_2}^v &= (1 - q)\phi P_2^v + (1 - q_1)\mu I_{A_0}^v + (\mu/2)I_{A_1}^v - \nu I_{A_2}^v - \gamma I_{A_2}^v - \rho_a^v I_{A_2}^v + q_v p I_{A_2}^u \\
\dot{I}_{A_M}^v &= \rho_a^v (I_{A_0}^v + I_{A_1}^v + I_{A_2}^v) + (1 - q_v)\phi P_M^v - \gamma I_{A_M}^v \\
\dot{R}_{S_0}^v &= \gamma I_{S_0}^v + q_v p R_{S_0}^u - w_I R_{S_0}^v - \mu R_{S_0}^v + (\nu/2)R_{S_1}^v + \nu(1 - q_2)R_{S_2}^v \\
\dot{R}_{S_1}^v &= \gamma I_{S_1}^v + q_v p R_{S_1}^u - w_I R_{S_1}^v + \mu q_1 R_{S_0}^v - (\mu/2)R_{S_1}^v - (\nu/2)R_{S_1}^v + \nu q_2 R_{S_2}^v \\
\dot{R}_{S_2}^v &= \gamma I_{S_2}^v + q_v p R_{S_2}^u - w_I R_{S_2}^v + (\mu/2)R_{S_1}^v + \mu(1 - q)R_{S_0}^v - \nu_2 R_{S_2}^v \\
\dot{R}_{S_M}^v &= \gamma I_{S_M}^v + q_v p R_{S_M}^u - w_I R_{S_M}^v \\
\dot{R}_{A_0}^v &= \gamma I_{A_0}^v + q_v p R_{A_0}^u - w_I R_{A_0}^v - \mu R_{A_0}^v + (\nu/2)R_{A_1}^v + \nu_2(1 - q_2)R_{A_2}^v \\
\dot{R}_{A_1}^v &= \gamma I_{A_1}^v + q_v p R_{A_1}^u - w_I R_{A_1}^v + \mu q_1 R_{A_0}^v - (\mu/2)R_{A_1}^v - (\nu/2)R_{A_1}^v + \nu q_2 R_{A_2}^v \\
\dot{R}_{A_2}^v &= \gamma I_{A_2}^v + q_v p R_{A_2}^u - w_I R_{A_2}^v + (\mu/2)R_{A_1}^v + \mu(1 - q)R_{A_0}^v - \nu R_{A_2}^v \\
\dot{R}_{A_M}^v &= \gamma I_{A_M}^v + q_v p R_{A_M}^u - w_I R_{A_M}^v
\end{aligned} \tag{A.10}$$

#### 455 Perceived Induced Immunity

$$\begin{aligned}
\dot{S}_0^w &= -F_{S_0^w} - \mu S_0^w + (\nu/2)S_1^w + (1 - q_2)\nu S_2^w + (1 - q_v)p S_0^u + w_I (R_{S_0}^v + R_{S_0}^w + R_{A_0}^v + R_{A_0}^w + R_{A_M}^v \\
&\quad + R_{A_M}^w + R_{S_M}^v + R_{S_M}^w + R_{A_M}^u) - w S_0^w + w'_I S_0^v \\
\dot{S}_1^w &= -F_{S_1^w} - (\mu/2)S_1^w + q_1\mu S_0^w - (\nu/2)S_1^w + q_2\nu S_2^w + (1 - q_v)p S_1^u + w_I (R_{S_1}^v + R_{S_1}^w + R_{A_1}^v + R_{A_1}^w) \\
&\quad - w S_1^w + w'_I S_1^v \\
\dot{S}_2^w &= (1 - q_1)\mu S_0^w + (\mu/2)S_1^w - \nu S_2^w + (1 - q_v)p S_2^u + w_I (R_{S_2}^v + R_{S_2}^w + R_{A_2}^v + R_{A_2}^w) - w S_2^w + w'_I S_2^v \\
\dot{E}_0^w &= F_{W_0} - \mu E_0^w + (\nu/2)E_1^w + (1 - q_2)\nu E_2^w - \sigma E_0^w + (1 - q_v)p E_0^u - w E_0^w
\end{aligned}$$

Table 3: Force of Infections

| Infectious  |  |
|---|--|
| $(I_{S_0}^u + I_{S_0}^s + I_{S_0}^w) + \alpha(P_0^u + I_{A_0}^u + P_0^v + I_{A_0}^v + P_0^w + I_{A_0}^w) + \delta(P_1^u + I_{A_1}^u + P_1^v + I_{A_1}^v + P_1^w + I_{A_1}^w) + \delta(I_{S_1}^u + I_{S_1}^v + I_{S_1}^w)$ |  |
| $F_{\xi_0} = \frac{N_{crit}\beta\xi_0}{N}(\text{Infectious}), \xi_0 = S_0^u, S_0^w, \varepsilon S_0^v$  | $F_{\xi_1} = \frac{N_{crit}\delta\beta\xi_1}{N}(\text{Infectious}), \xi_1 = S_1^u, S_1^v, \varepsilon S_1^w$ |

$$\begin{aligned}
 \dot{E}_1^w &= F_{W_1} - (\mu/2)E_1^w + q_1\mu E_0^w - (\nu/2)E_1^w + q_2\nu E_2^w - \sigma E_1^w + (1 - q_v)pE_1 - wE_1^w \\
 \dot{E}_2^w &= (1 - q_1)\mu E_0^w + (\mu/2)E_1^w - \nu E_2^w - \sigma E_2^w + (1 - q_v)pE_2 - wE_2^w \\
 \dot{P}_0^w &= \sigma E_0^w - \mu P_0^w + (\nu/2)P_1^w + (1 - q_2)\nu P_2^w - \phi P_0^w - \rho_a^v P_0^w + (1 - q_v)pP_0 - wP_0^w \\
 \dot{P}_1^w &= \sigma E_1^w - (\mu/2)P_1^w + q_1\mu P_0^w - (\nu/2)P_1^w + q_2\nu P_2^w - \phi P_1^w - \rho_a^v P_1^w + (1 - q_v)pP_1 - wP_1^w \\
 \dot{P}_2^w &= \sigma E_2^w + (1 - q_1)\mu P_0^w + (\mu/2)P_1^w - \nu P_2^w - \phi P_2^w - \rho_a^v P_2^w + (1 - q_v)pP_2 - wP_2^w \\
 \dot{P}_M^w &= \rho_a^v(P_0^w + P_1^w + P_2^w) - \phi P_M^w - wP_M^w \\
 \dot{I}_{S_0}^w &= q\phi P_0^w - \mu I_{S_0}^w - \gamma I_{S_0}^w - \rho_s^v I_{S_0}^w - wI_{S_0}^w \\
 \dot{I}_{S_1}^w &= q\phi P_1^w + q_I\mu I_{S_0}^w - \gamma I_{S_1}^w - \rho_s^v I_{S_1}^w - wI_{S_1}^w \\
 \dot{I}_{S_2}^w &= q\phi P_2^w + (1 - q_I)\mu I_{S_0}^w - \gamma I_{S_2}^w - \rho_s^v I_{S_2}^w - wI_{S_2}^w \\
 \dot{I}_{S_M}^w &= \rho_s^v(I_{S_0}^w + I_{S_1}^w + I_{S_2}^w) + q\phi P_M^w - \gamma I_{S_M}^w - wI_{S_M}^w \\
 \dot{I}_{A_0}^w &= (1 - q)\phi P_0^w - \mu I_{A_0}^w + (\nu/2)I_{A_1}^w + (1 - q_2)\nu I_{A_2}^w - \gamma I_{A_0}^w - \rho_a^v I_{A_0}^w + (1 - q_v)pI_{A_0} - wI_{A_0}^w \\
 \dot{I}_{A_1}^w &= (1 - q)\phi P_1^w - \mu I_{A_1}^w + q_1\mu I_{A_0}^w - (\nu/2)I_{A_1}^w + q_2\nu I_{A_2}^w - \gamma I_{A_1}^w - \rho_a^v I_{A_1}^w + (1 - q_v)pI_{A_1} - wI_{A_1}^w \\
 \dot{I}_{A_2}^w &= (1 - q)\phi P_2^w + (1 - q_1)\mu I_{A_0}^w + (\mu/2)I_{A_1}^w - \nu_2 I_{A_2}^w - \gamma I_{A_2}^w - \rho_a^v I_{A_2}^w + (1 - q_v)pI_{A_2} - wI_{A_2}^w \\
 \dot{I}_{A_M}^w &= \rho_a^v(I_{A_0}^w + I_{A_1}^w + I_{A_2}^w) + (1 - q)\phi P_M^w - \gamma I_{A_M}^w - wI_{A_M}^w \\
 \dot{R}_{S_0}^w &= \gamma I_{S_0}^w + (1 - q_v)pR_{S_0}^u - w_I R_{S_0}^w - w R_{S_0}^w - \mu R_{S_0}^w + (\nu/2)R_{S_1}^w + \nu(1 - q_2)R_{S_2}^w \\
 \dot{R}_{S_1}^w &= \gamma I_{S_1}^w + (1 - q_v)pR_{S_1}^u - w_I R_{S_1}^w - w R_{S_1}^w + \mu q_1 R_{S_0}^w - (\mu/2)R_{S_1}^w - (\nu/2)R_{S_1}^w + \nu q_2 R_{S_2}^w \\
 \dot{R}_{S_2}^w &= \gamma I_{S_2}^w + (1 - q_v)pR_{S_2}^u - w_I R_{S_2}^w - w R_{S_2}^w + (\mu/2)R_{S_1}^w + \mu(1 - q_1)R_{S_0}^w - \nu R_{S_2}^w \\
 \dot{R}_{S_M}^w &= \gamma I_{S_M}^w + (1 - q_v)pR_{S_M}^u - w_I R_{S_M}^w - w R_{S_M}^w \\
 \dot{R}_{A_0}^w &= \gamma I_{A_0}^w + (1 - q_v)pR_{A_0}^u - w_I R_{A_0}^w - w R_{A_0}^w - \mu R_{A_0}^w + (\nu/2)R_{A_1}^w + \nu(1 - q_2)R_{A_2}^w \\
 \dot{R}_{A_1}^w &= \gamma I_{A_1}^w + (1 - q_v)pR_{A_1}^u - w_I R_{A_1}^w - w R_{A_1}^w + \mu q_1 R_{A_0}^w - (\mu/2)R_{A_1}^w - (\nu/2)R_{A_1}^w + \nu q_2 R_{A_2}^w \\
 \dot{R}_{A_2}^w &= \gamma I_{A_2}^w + (1 - q_v)pR_{A_2}^u - w_I R_{A_2}^w - w R_{A_2}^w + (\mu/2)R_{A_1}^w + \mu(1 - q)R_{A_0}^w - \nu R_{A_2}^w \\
 \dot{R}_{A_M}^w &= \gamma I_{A_M}^w + (1 - q_v)pR_{A_M}^u - w_I R_{A_M}^w - w R_{A_M}^w
 \end{aligned} \tag{A.11}$$

456 Where  $\{F_{S_0}^u, F_{S_1}^u, F_{S_0}^v, F_{S_1}^v, F_{S_0}^w, F_{S_1}^w\}$  are force of infections and defined in Table 3.

| Parameter                    | Definition  | Value                   | Reference    |
|------------------------------|---|-------------------------|--------------|
| $R_0$                        | Basic reproduction number   | 2.4                     | [20]         |
| $\beta$                      | Transmission rate   | 0.223                   | Calculated   |
| $\sigma$                     | Latent period   | 2 days <sup>-1</sup>    | [20]         |
| $\phi$                       | Pre-symptomatic period  | 4.6 days <sup>-1</sup>  | [20]         |
| $\gamma$                     | Infectious period   | 10 days <sup>-1</sup>   | [20]         |
| $\delta$                     | Reduction in transmission due to social distancing in class 1   | 0.25                    | Chosen       |
| $\alpha$                     | Reduction in transmission due to being asymptomatic   | 0.5                     | Chosen       |
| $Q$                          | Proportion of infected individuals who show symptoms  | 0.69                    | Median value |
| $\mu_{\max}$                 | Maximal rate at which an un-vaccinated individual transitions from a less socially distant class to a more socially distant class | 1 days <sup>-1</sup>    | Chosen       |
| $\mu_{\max}^v, \mu_{\max}^w$ | Maximal rate at which a vaccinated individual transitions from a less socially distant class to a more socially distant class     | 0.5 days <sup>-1</sup>  | Chosen       |
| $\nu_{\max}$                 | Maximal rate at which an un-vaccinated individual moves from a more socially distant class to a less socially distant class       | 1 days <sup>-1</sup>    | Chosen       |
| $\nu_{\max}^v, \nu_{\max}^w$ | Maximal rate at which a vaccinated individual moves from a more socially distant class to a less socially distant class           | 2 days <sup>-1</sup>    | Chosen       |
| $\mu_I$                      | Rate at which people showing symptoms choose to isolate   | 0.01 days <sup>-1</sup> | Chosen       |
| $q_0$                        | Proportion of $S_0$ socially distancing into $S_1$  | 0.9                     | Chosen       |
| $q_2$                        | Proportion of $S_2$ relaxing social distancing into $S_1$   | 0.6                     | Chosen       |
| $q_I$                        | Proportion of symptomatic individuals $I_{S_0}$ who isolate into $I_{S_1}$  | 0.6                     | Chosen       |
| $C_c$                        | Critical cost to induce social relaxation   | 50 days                 | Chosen       |
| $C_0$                        | Cost that leads to half the maximal rate of social relaxation   | 100 days                | Chosen       |

Table 4: Values of the model parameters.

Table 5: Model Parameters

| Fixed parameters |   |             |         |
|------------------|---|-------------|---------|
| parameter        | Definition  | Value       | comment |
| $q_v$            | $(1 - q_v)$ is the fraction of people with perceived induced immunity | 1           | Chosen  |
| $\rho_a^v$       | Testing rate of vaccinated people                                     | $0.5\rho_a$ | Chosen  |
| $\varepsilon$    | $(1 - \varepsilon)$ is the efficacy of the vaccine                    | 0.0         | Chosen  |
| $\omega_W$       | Media waning rate   | 0.07        | Chosen  |
| $\omega_I$       | Disease waning rate   | 0.005       | Chosen  |
| $\omega_V$       | Vaccine waning rate   | 0.005       | Chosen  |